Early-Life Insults Impair Parvalbumin Interneurons via Oxidative Stress: Reversal by *N*-Acetylcysteine

Jan-Harry Cabungcal, Pascal Steullet, Rudolf Kraftsik, Michel Cuenod, and Kim Q. Do

Background: A hallmark of the pathophysiology of schizophrenia is a dysfunction of parvalbumin-expressing fast-spiking interneurons, which are essential for the coordination of neuronal synchrony during sensory and cognitive processing. Oxidative stress as observed in schizophrenia affects parvalbumin interneurons. However, it is unknown whether the deleterious effect of oxidative stress is particularly prevalent during specific developmental time windows.

Methods: We used mice with impaired synthesis of glutathione (*Gclm* knockout [KO] mice) to investigate the effect of redox dysregulation and additional insults applied at various periods of postnatal development on maturation and long-term integrity of parvalbumin interneurons in the anterior cingulate cortex.

Results: A redox dysregulation, as in *Gclm* KO mice, renders parvalbumin interneurons but not calbindin or calretinin interneurons vulnerable and prone to exhibit oxidative stress. A glutathione deficit delays maturation of parvalbumin interneurons, including their perineuronal net. Moreover, an additional oxidative challenge in preweaning or pubertal but not in young adult *Gclm* KO mice reduces the number of parvalbumin-immunoreactive interneurons. This effect persists into adulthood and can be prevented with the antioxidant *N*-acetylcysteine.

Conclusions: In *Gclm* KO mice, early-life insults inducing oxidative stress are detrimental to immature parvalbumin interneurons and have long-term consequences. In analogy, individuals carrying genetic risks to redox dysregulation would be potentially vulnerable to early-life environmental insults, during the maturation of parvalbumin interneurons. Our data support the need to develop novel therapeutic approaches based on antioxidant and redox regulator compounds such as *N*-acetylcysteine, which could be used preventively in young at-risk subjects.

Key Words: Anterior cingulate cortex, gene-environment interactions, glutamate cysteine ligase, glutathione, parvalbumin, schizophrenia

Converging evidence suggests that a redox dysregulation due to genetic and/or environmental factors might contribute to schizophrenia pathophysiology. Oxidative stress and abnormal levels of antioxidants, including reduced levels of glutathione (GSH), a major antioxidant and redox regulator, are observed in peripheral tissue and central nervous system of patients (1,2). The implication of redox dysregulation in the pathology is supported by the beneficial effect of the redox regulator and GSH precursor *N*-acetylcysteine (NAC) on schizophrenia patients (3–5). This redox dysregulation can have a genetic origin. Impaired upregulation of GSH synthesis is observed in patients carrying risk variants in the gene for the catalytic subunit of glutamate cysteine ligase (GCL), the rate-limiting enzyme of GSH synthesis (6). Moreover, abnormal function of proteins encoded by well-replicated susceptibility genes (*PRODH, DISC1, G72, DTNBP1, NRG1*) also causes oxidative stress and/or hypersensitivity to oxidative stress (7–11). Thus, a genetic susceptibility to redox dysregulation could render individuals vulnerable to the impact of additional environmental insults, known to generate oxidative stress and affect antioxidant systems (1). We hypothesize, on the basis of the concept that schizophrenia has a neurodevelopmental component (12), that a redox dysregulation caused by genetic susceptibilities and environmental insults during development could contribute to the emergence of the disease.

Among well-replicated observations on the pathophysiology of schizophrenia are anomalies in parvalbumin-expressing fast-spiking interneurons (PVI) and their synaptic connections to pyramidal neurons (13). Fast-spiking interneurons control the output of principal neurons and are necessary for γ neuronal synchrony, facilitating information processing during sensory perception and cognitive tasks (14–16). Abnormal γ oscillations during cognitive and sensory tasks in patients further support a dysfunction of these interneurons in schizophrenia (17–20). Studies in rodents show that PVI are sensitive to severe psychosocial stress such as maternal separation (21) and social isolation (22,23). The PVI impairment after these environmental trauma could be mediated by oxidative stress. Indeed, social isolation and ketamine administration affect PVI via superoxide overproduction (22,24). Interestingly, decreased GSH levels (25,26), sign of oxidative stress (27), reduced parvalbumin (PV) expression (28), and PVI number (29) are reported in prefrontal cortex of patients. These suggest that a redox dysregulation might contribute to PVI defects. Presently unknown, however, is whether PVI impairment results from early-life disturbances or arises later on onset or in the course of the illness. In this context, it was important to assess PVI vulnerability to oxidative stress along various stages of their maturation. In rodent models, PVI start to express PV after the first postnatal week (30,31). While they develop chemical and electrical connections, they acquire fast-spiking properties after 2–3 weeks (32). They undergo further developmental changes at adolescence (second month), including changes in dopamine modulation of their

From the Department of Psychiatry (J-HC, PS, MC, KQD), Center for Psychiatric Neuroscience, Centre Hospitalier Universitaire Vaudois; and University of Lausanne; and the Department of Fundamental Neurosciences (RK), University of Lausanne, Lausanne, Switzerland.

Address correspondence to Kim Quang Do, Ph.D., Department of Adult Psychiatry, Center for Psychiatric Neuroscience, Centre Hospitalier Universitaire Vaudois and University of Lausanne, Route de Cery, Prilly-Lousanne CH-1008, Switzerland; E-mail: kim.do@chuv.ch.

Received Jul 4, 2012; revised Sep 24, 2012; accepted Sep 24, 2012.

0006-3223/$36.00
http://dx.doi.org/10.1016/j.biopsych.2012.09.020

excitability (33) and in expression of *N*-methyl-D-aspartate and calcium ion-permeable α-Amino-3-hydroxy-5-methyl-4-isoxazole propionic acid receptors (34). During this maturation process, a specialized extracellular matrix, the perineuronal net (PNN), also forms around these interneurons (35) to promote maturation and synaptic and network stability (36).

To study the existence of vulnerability period(s) to redox dysregulation in PVI, we investigated these interneurons in mice with a genetically impaired GSH synthesis (*Gclm* knockout [KO] mice). These mice have 60%–70% decreased brain GSH contents (37,38), because they do not express GCLM, the modulatory subunit of GCL. This is a valid animal model, because deficit in GSH (25,26) and genetic association between *GCLM* and schizophrenia (39) have been reported. We investigated whether impaired GSH synthesis affected PVI maturation in the anterior cingulate cortex (ACC) and whether additional exogenous stress applied during specific developmental periods had deleterious and long-term effects on these interneurons. The ACC is indeed sensitive to early-life stress (40–43) and is affected in schizophrenia patients (44). Moreover, oxidative stress (27) and anomalies of non-pyramidal neurons are reported in ACC of patients (45). Finally, we explored whether PVI could be protected by an antioxidant.

Methods and Materials

Animals

Gclm KO mice (B6.129-*Gclm*^{tm1Tdal}) were provided by T. Dalton (University of Cincinnati) (46). *Gclm* KO mice were backcrossed with C57BL/6J mice over >10 generations. Mice were housed under a 12-hour light-dark cycle in groups of 3–5 individuals/cage. All breeding mice were obtained from heterozygotes (HZ × HZ). Experimental *Gclm* KO mice were from breeding individuals (males KO × females HZ), and control *Gclm* WT mice were from breeding individuals (WT × WT). Experiments were performed on males and were approved by the Local Veterinary Office.

Induction of an Additional Oxidative Stress During Various Developmental Periods

A pharmacological approach was chosen to generate additional oxidative insult in regions richly innervated by dopaminergic neurons (i.e., prefrontal cortex including ACC). This was accomplished by administration of a specific inhibitor of the dopamine reuptake transporter, GBR-12909 (GBR). The GBR-12909 (BioTrend, Zurich, Switzerland) was injected (SC 5 mg/kg) daily, between postnatal days 10–20 (preweaning), or 30–40 (pubertal), or 80–90 (young adult). Phosphate buffer saline (PBS) was used for control injection.

NAC Treatment

Fresh solution (1 g/L) of NAC (Sigma-Aldrich, St. Gallen, Switzerland), a precursor of GSH with antioxidant properties (47), was provided as drinking water to pregnant females and lactating mothers and their offspring until sacrifice (at day 40). The NAC solution was renewed every other day. In addition, NAC was injected into pups (SC 1 g/kg) daily from day 5 to 10, a period in which PV expression begins.

Immunohistochemistry and Stereological Quantification of PVI

Mice were anesthetized and perfused, and their brains were fixed (48). Coronal frozen sections (40 μm) were used to investigate the ACC and primary somatosensory cortex (SM1). Brain sections were immunolabeled for PV as in Steullet *et al.* (38) and Cabungcal *et al.* (48). Cell density count of PVI was quantified in the ACC and SM1 with the StereoInvestigator 7.5 software (MBF Bioscience, Williston, Vermont) (38). Stereological counting started with low magnification (2.5× objective) to identify the boundaries of the region of interest (ROI) on 2–4 consecutive sections from each animal. The ACC (at Bregma approximately 1.3–1.4) was delineated from the boundaries of infralimbic and secondary motor cortices after the anatomical cytoarchitectonic areas given by Franklin and Paxinos (49). This included the cingulate cortex area 1 (cg1) and part of area 2 (cg2). A small intermediate zone was created between these three regions, to ensure that the ROI in the ACC did not overlap with infralimbic and secondary motor cortices. An optical dissector (counting box) within the section thickness and sampling frames adapted for the ACC and SM1 were used to analyze and count neurons (50). The optical dissector boxes (40 × 40 μm with a depth of 15 μm) were placed by the software in each sampling frame starting from a random point inside the ROI of the ACC or SM1. Counting was carried out with higher magnification (40× objective). The PVI were counted when they were in focus at the surface of the box until they were out of focus at 15-μm depth of the counting box. A 5-μm guard zone was used to avoid artifacts caused by tissue shrinkage due to the immune-preparation process. Because the ACC and SM1 differed in their size, the volume of brain sections analyzed was not equal for each region. In ACC of 10- and 20-day-old mice, 24 counting frames were used, whereas quantification in SM1 required 37 frames. The number of frames was increased to 26 in ACC of 40- and 90-day-old mice. The mean numbers of PVI/unit volume in the ACC (or SM1) were compared between genotypes or between treatments with *t* tests.

Immunofluorescence Staining, Confocal Microscopy, and Image Analysis

Oxidative stress was visualized with a mouse monoclonal primary antibody against 8-oxo-7,8-dihydro-20-deoxyguanine (8-oxo-dG), a DNA adduct formed by the reaction of hydroxyl radicals with the DNA guanine base (51). To assess 8-oxo-dG labeling in various types of interneurons, brain sections containing the ACC were incubated for 48 hours with rabbit polyclonal anti-PV, anti-calbindin-28k (anti-CB), or anti-calretinin (anti-CR) (1:2500; Swant, Marly, Fribourg, Switzerland) primary antibodies together with the mouse monoclonal anti-8-oxo-dG (1:350; AMS Biotechnology, Bioggio-Lugano, Switzerland) primary antibody. To visualize the PNN that specifically surrounds PVI, sections were incubated in a solution containing the biotin-conjugated lectin *Wisteria floribunda agglutinin* (WFA). Briefly, sections were first incubated with PBS + Triton .3% + sodium azide (1 g/L) containing 2% normal horse serum, followed by 48-hour incubation with rabbit polyclonal anti-PV (1:2500; Swant) and biotin conjugated-WFA (1:2000; Sigma). Sections were then washed, incubated with their appropriate fluorescent secondary antibodies (goat antimouse immunoglobulin G [1:300; Alexa Fluor 488; Molecular Probes, Eugene, Oregon], antirabbit immunoglobulin G [1:300; CY3; Chemicon International, Temecula, California], CY2-streptabidin [1:300]), and counterstained with 100 ng/mL DAPI (4′-6-diamidino-2-phenylindole; Vector Laboratories, Burlingame, California). Sections were visualized with a Zeiss confocal microscope with Plan-NEOFLUAR objectives. All peripherals were controlled with LSM 510 software (Carl Zeiss AG, Feldbach, Switzerland). Z stacks of nine images (with a 2.13-μm interval) were scanned (1024 × 1024 pixels) for analysis with IMARIS 7.3 software (Bitplane AG, Zurich, Switzerland). Images were filtered with a Gaussian filter to remove

unwanted background noise and sharpen cell profile contours. An ROI as defined in the stereological procedure was created in the ACC. The ROI was masked throughout the Z stacks to isolate regional subvolumes of the ACC in which the numbers of PV-, CB- and CR-expressing interneurons were quantified. This quantification method gave qualitatively similar results as the stereological method. To quantify the overall 8-oxo-dG, the staining intensity and number of labeled voxels within the ROI were measured. To quantify 8-oxo-dG in each type of interneurons, we used the Coloc module of the IMARIS software to calculate the proportion of all PV-immunolabeled voxels (respectively, CR- and CB-immunolabeled voxels) which were 8-oxo-dG-immunolabeled. Coloc gives the count of colocalized voxels between the immunolabeled profiles of interest. To analyze the number of PVI surrounded by WFA-labeled PNN, we used the spots module to assign spot markings on the profile-labeled voxels that fall within a given size. Briefly, the channels for PV and WFA immunolabeling were chosen, and the profile size criterion (>9 and 5 μm, respectively) was defined to quantify stained profiles above these given sizes. The procedure was visually monitored/verified before proceeding. Spots generated for PV that contacted/overlapped with spots generated for WFA were considered as those PVI surrounded by PNN (WFA-positive PVI). We also assessed PNN by quantifying the overall intensity of WFA-immunolabeling (in arbitrary unit). The mean number of PVI, WFA-positive PVI, CR and CB-immunolabeled cells, and the overall 8-oxo-dG- and WFA-labeling were compared between the two genotypes and treatments (when applied) with multivariate analysis of variance (ANOVA) followed by a Dunnett test. The significance level for type 1 error was set at $p < .05$. Pair-wise comparisons were also performed with *t* test, and the degrees of freedom, *t* ratio, and *p* values are provided in the results. In the text and when applied, the *p* values that are significant after Bonferroni correction for multiple comparisons are indicated with an asterisk (*).

Results

Oxidative Stress and Delayed PVI Maturation in ACC of *Gclm* KO Mice

We first investigated whether low brain GSH content was sufficient to induce oxidative stress in the ACC. The degree of oxidative stress was assessed with an antibody against 8-oxo-dG, a marker for DNA oxidative damage (51). In all investigated ages (preweaning at days 10 [P10] and 20 [P20], pubertal at day 40 [P40], and young adult at day 90 [P90]), we observed a significantly higher 8-oxo-dG labeling in the ACC of *Gclm* KO compared with WT mice (Figure S1 in Supplement 1) [P10: $t(7.6) = -5.6$, $p < .001$; P20: $t(4) = -2.3$, $p = .04$; P40: $t(5.9) = -2.9$, $p = .01$; P90: $t(3.8) = -2.7$, $p = .03$]. The extranuclear localization of the labeling suggested oxidative damage of mitochondrial DNA. We then investigated the maturation and integrity of PVI throughout postnatal development. With a stereological quantification, we found that the number of cells expressing PV (PVI) was significantly lower in KO compared with WT mice only during early PVI development [at P10: $t(9.4) = 12.7$, $p < .001$] but not in later stages (P20, P40, P90) (Table 1). This suggested that PVI were quite resistant to a GSH deficit, although their maturation was delayed. We further assessed a later stage of maturation by quantifying the number PVI surrounded by PNN. The presence of well-formed PNN around PVI constitutes indeed a late marker of PVI maturation. We performed double-immunofluorescent labeling for PV and WFA, a lectin that recognizes PNN around PVI (Figure 1). We did not observe, as with the stereological method, a difference in the number of PVI between the two genotypes at days 20, 40, and 90 (Figure 1B). However, the number of WFA-positive PVI was significantly lower in 20- [$t(3.8) = 3.6$, $p = .01$] and 40- [$t(6.4) = 2.3$, $p = .05$] but not 90-day-old ($p = .7$) KO compared with age-matched WT mice (Figure 1C). The overall intensity of WFA labeling was also significantly lower in 20- and 40-day-old KO compared with age-matched WT mice (Table S1 in Supplement 1). This indicated that, although PVI in ACC were quite resistant to a GSH deficit and to

Table 1. Stereological Count of PVI in the ACC of *Gclm* KO and WT Mice

	PVI Number (mean ± SD)	
Postnatal Age	WT	KO
Day 10	5.8 ± .6 ($n = 4$)	3.3 ± .5[a] ($n = 4$)
Day 20	24.5 ± 6.2 ($n = 4$)	22 ± 2.4 ($n = 4$)
Day 40	20.1 ± 4.5 ($n = 5$)	19.6 ± 4 ($n = 5$)
Day 90	20 ± 3.7 ($n = 4$)	19.7 ± 4.1 ($n = 4$)

Stereological count of parvalbumin-immunoreactive interneurons (PVI) in the anterior cingulate cortex (ACC) of *Gclm* knockout (KO) and wild-type (WT) mice at postnatal day (P)10, P20, P40, and P90.

[a]Significant difference between genotypes at $p < .001$ level.

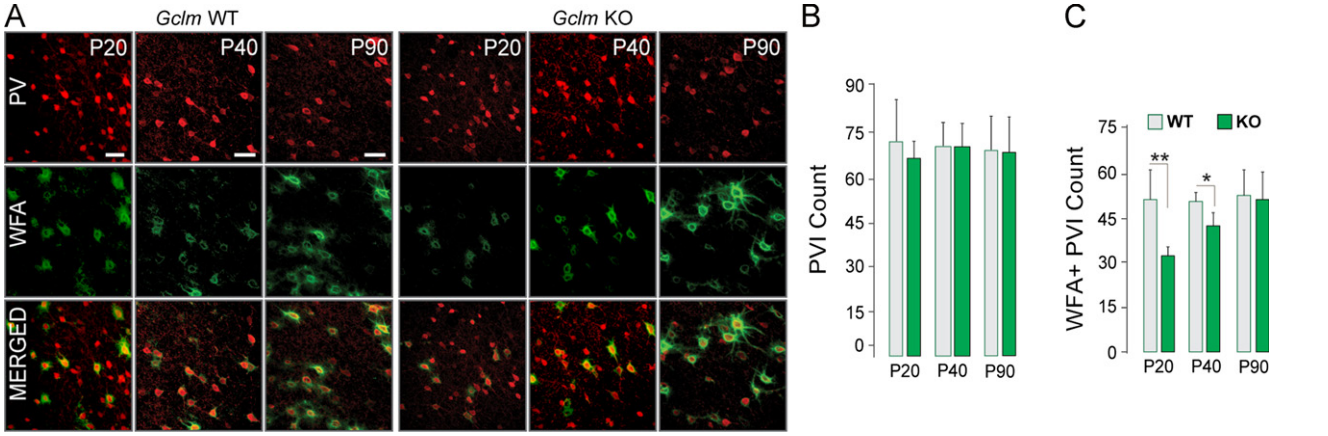

Figure 1. Delayed formation of perineuronal net (PNN) around parvalbumin-immunoreactive interneurons (PVI) in the anterior cingulate cortex of *Gclm* knockout (KO), compared with wild-type (WT) mice. **(A)** Micrographs show double labeling for parvalbumin (PV) and *Wisteria floribunda agglutinin* (WFA) (labels PNN around PVI) in the anterior cingulate cortex of both genotypes. Scale: 40 μm. **(B)** Number of PVI ± SD. For each group, $n = 4–5$. **(C)** Number of PVI surrounded by PNN (WFA+ PVI) ± SD. For each group, $n = 4–5$. $^{**}p < .01$; $^{*}p < .05$. P, postnatal day.

the resulting oxidative stress, they exhibited a delayed maturation, as particularly evidenced by the delayed formation of PNN.

GBR-Induced Increase in Oxidative Stress Affects PVI in Young But Not Adult *Gclm* KO Mice

To model the oxidative stress that could be generated by environmental insults, we injected mice with a specific dopamine reuptake inhibitor (GBR), during preweaning (P10 to P20), pubertal (P30 to P40), or early adult (P80 to P90) stages. The GBR increases extracellular dopamine, producing reactive oxygen species through its catabolism and auto-oxidation (2,52,53). This pharmacological approach partially mimics the prefrontal dopamine release during psychosocial stress (54,55). The GBR significantly increased 8-oxo-dG labeling in the ACC of KO [P20: $t(3.6) = 2.2$, $p = .05$; P40: $t(5.2) = -2.0$, $p = .05$; P90: $t(1.6) = 5.8$, $p = .01$] but not WT mice (Figure 2), regardless of the injection period. This indicated that dopamine excess induced additional oxidative stress only in KO. The GBR had no effect on the number of PVI in WT mice (Figure 3C), whereas it decreased PVI number in preweaning [P20: $t(7.9) = 4.3$, $p = .002$] and pubertal [P40: $t(17.9) = 3.3$, $p = .002$] KO mice (Figure 3B). Because GBR did not cause oxidative stress and did not affect PVI in WT mice, this indicated that the deleterious effect of GBR in young KO mice was associated with the induced oxidative stress and not due to other dopamine-mediated action. By contrast, GBR administrated in young adult KO mice did not affect PVI number [P90: $t(15.9) = .9$, $p = .7$], although it significantly increased oxidative stress. Finally, GBR treatment during preweaning age did not affect PVI number in the SM1 of KO mice (Figure S2 in Supplement 1), a cortical region weakly innervated by dopaminergic neurons (56). Together, these experiments revealed that PVI are vulnerable to oxidative stress, particularly during their development.

PVI—Not CB and CR Interneurons—Are Vulnerable to Redox Dysregulation and Prone to Oxidative Stress

We then checked whether a redox dysregulation and GBR challenge also affected other types of interneurons in the ACC. The number of CB- or CR-expressing interneurons was not altered by GBR in KO mice (Figure S3 in Supplement 1). In addition, 8-oxo-dG labeling in CB- or CR-expressing interneurons did not vary significantly with genotype or treatment (Figure 4). By contrast, the 8-oxo-dG labeling in PVI varied significantly with genotype [ANOVA, $F(1,15) = 15.31$, $p = .002$] and treatment [$F(1,15) = 17.47$, $p = .001$], with the strongest labeling in PVI of KO mice treated with GBR (Figures 4B and C). More 8-oxo-dG colocalized with PVI voxels in GBR-treated compared with PBS-treated KO mice [$t(6.0) = -3.1$, $p = .01$*].

Redox Dysregulation During Early Postnatal Development Causes Long-Term Impairment of PVI Integrity

As shown in the preceding text, GBR-induced increase of oxidative stress in preweaning KO mice (Figures 2B, D and 4B, C) was associated with a decreased PVI number immediately after the end of the GBR treatment (Figure 3A, B). We assessed whether this impairment was only transient or remained until adulthood. In young adult mice treated during their preweaning

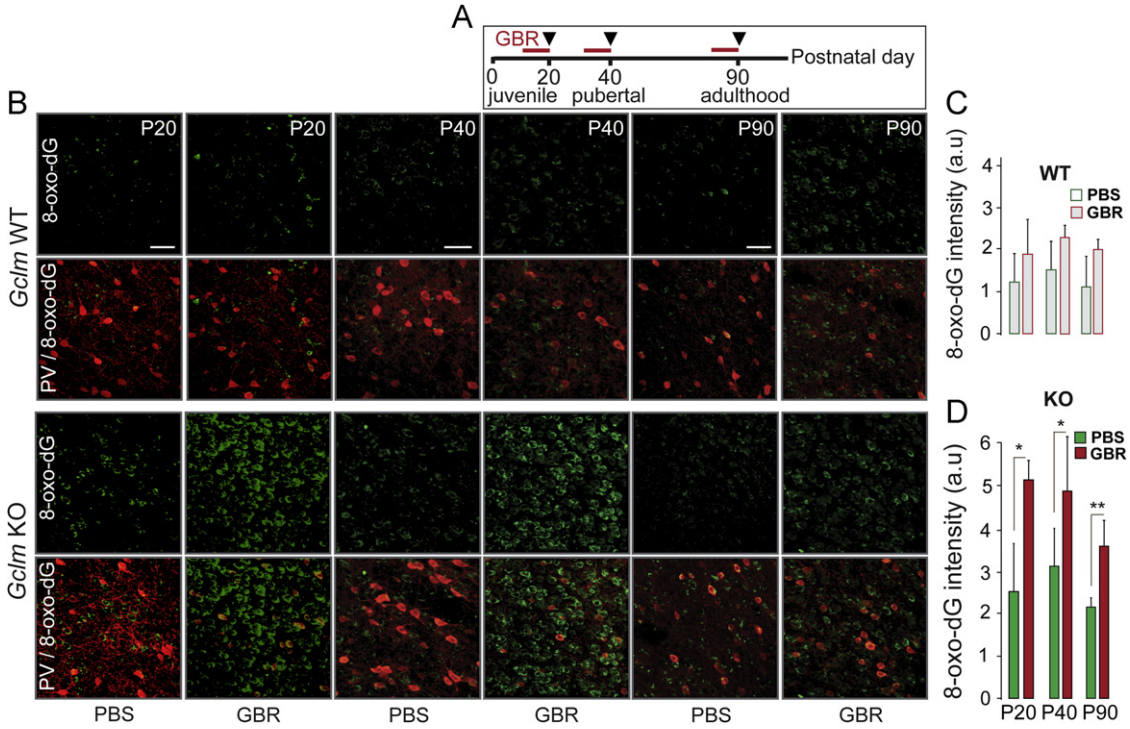

Figure 2. Administration of the dopamine reuptake inhibitor GBR-12909 (GBR) significantly increases 8-oxo-dG labeling in the anterior cingulate cortex (ACC) of *Gclm* KO but not WT mice. **(A)** Experimental design. Mice were treated with GBR (or phosphate buffer saline [PBS]) at various postnatal ages (from P10 to 20), or (from P30 to 40), or (from P80 to 90). The red horizontal lines indicate periods of treatment; arrowheads indicate the respective times of sacrifice (at P20, P40, P90) for each mice group. **(B)** Micrographs show double labeling for PV and 8-oxo-dG in the ACC of mice of both genotypes treated with either GBR or PBS at preweaning (see P20), pubertal (see P40), or young adult (see P90) age. Note the prominent 8-oxo-dG labeling in GBR-treated *Gclm* KO mice. Scale: 40 μm. **(C)** 8-oxo-dG labeling in arbitrary unit (a.u.) ± SD in WT mice. For each group, $n = 4$–5. **(D)** 8-oxo-dG labeling in arbitrary unit (a.u.) ± SD in *Gclm* KO mice. For each group, $n = 4$–5. **$p < .01$; *$p < .05$. Abbreviations as in Figure 1.

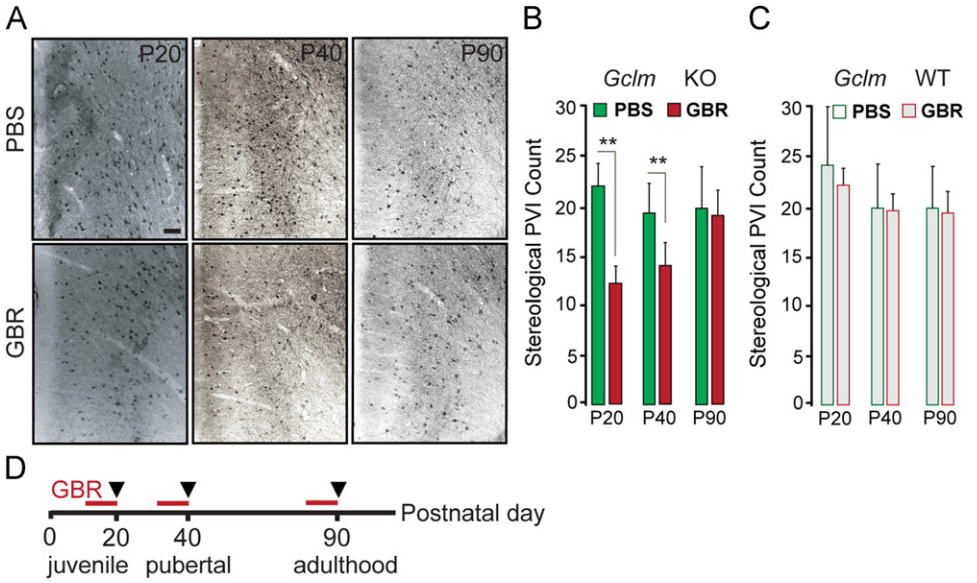

Figure 3. Administration of GBR during preweaning (from P10 to 20) or pubertal (from P30 to 40) stage but not in young adult (from P80 to 90) decreases the number of PVI in the ACC of *Gclm* KO mice. **(A)** Micrographs illustrate parvalbumin (PV) labeling in the ACC of GBR- or PBS-treated *Gclm* KO mice. Scale: 80 μm. (**B**) Stereological count of PVI ± SD in *Gclm* KO mice. For each group, $n = 4$–5. $^{**}p < .01$. **(C)** Stereological count of PVI ± SD in WT mice. For each group, $n = 4$–5. **(D)** Experimental design. Mice were treated with GBR (or PBS) at various postnatal ages (from P10 to 20, P30 to 40, or P80 to 90). The red horizontal lines indicate periods of treatment; arrowheads indicate the respective times of sacrifice of each mice group. Abbreviations as in Figures 1 and 2.

age (P10 to P20) with either GBR or PBS, 8-oxo-dG labeling was significantly higher in KO compared with WT mice (Figure 5C) [ANOVA, $F(1,15) = 51.47$, $p < .0001$] but was lower than right after GBR treatment (see P20 KO mice in Figure 2D). This indicated that the additional oxidative stress induced by GBR in KO mice was transient. When assessing PVI and PNN, we found strong genotype ($p > .0001$) and treatment [for PVI: $F(1,15) = 5.96$, $p = .029$; for PNN: $F(1,15) = 10.84$, $p = .005$] effects. The number of PVI in PBS- and GBR-treated KO mice was significantly lower than in the matched WT groups (Figure 5D) [for PBS-treated: $t(6.0) = 3.8$, $p = .004$*; for GBR-treated: $t(5.9) = 4.7$, $p = .002$*]. Similarly, the number of PNN in PBS- and GBR-treated KO mice was significantly lower than in the matched WT groups (Figure 5E) [for PBS-treated: $t(4.8) = 2.6$, $p = .02$*; for GBR-treated: $t(6.9) = 9.4$, $p = .001$*]. Compared with preweaning PBS treatment, preweaning GBR treatment and its induced transient additional oxidative stress caused stronger long-term effect on PNN (Figure 5E) [$t(4.2) = 3.3$, $p = .01$*] and tended to affect PVI more (Figure 5D) [$t(6.7) = 2.2$, $p = .03$, nonsignificant]. These data revealed that PVI of mice with a redox dysregulation are highly vulnerable to early stressful manipulation that results in long-term PVI integrity impairment even after a preweaning challenge such as PBS injections.

NAC Prevents PVI Impairment Caused by GBR in *Gclm* KO Mice

In view of the detrimental consequences of oxidative stress on PVI during preweaning and pubertal ages, we assessed whether NAC—a cysteine precursor for GSH with antioxidant and redox regulator properties—could prevent PVI impairment in young KO mice. NAC, given throughout development until sacrifice (at P40), fully prevented the increase in 8-oxo-dG labeling induced by GBR (administered from P30 to P40) in KO mice (Figure 6A, B) [$t(3.1) = -4.3$, $p = .01$*]. Moreover, in PBS- and GBR-treated KO mice, NAC was able to lower 8-oxo-dG levels close to those found in WT mice (Figure 6B). Consequently, NAC prevented the GBR-induced PVI impairment (Figure 6A, C) [$t(16.3) = 3.3$, $p = .002$*] and PNN degradation (Figure 6A, D) [$t(4.3) = 8.3$, $p = .0004$*]. Thus, NAC re-established normal redox balance and ultimately protected PVI.

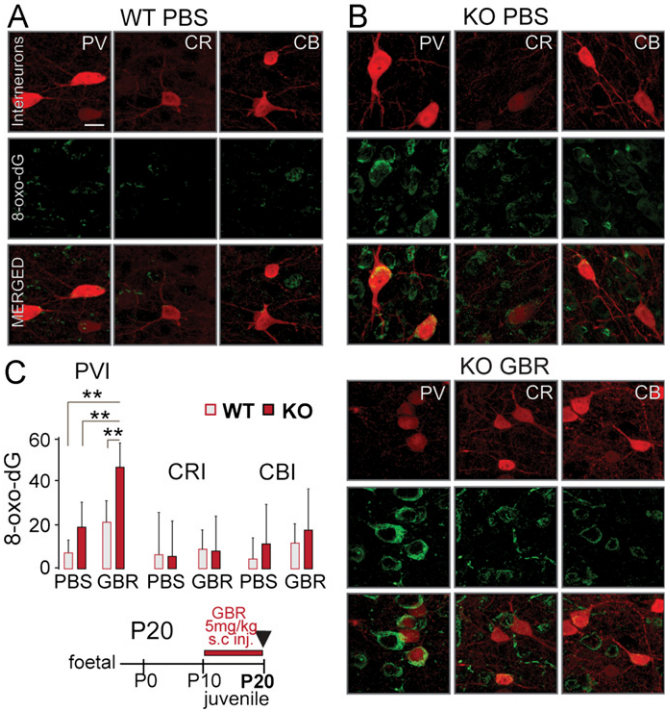

Figure 4. The PVI are more prone to display oxidative stress than calretinin (CRI) and calbindin (CBI) interneurons. **(A)** Micrographs show double labeling for 8-oxo-dG and one of the three interneuron markers (PV, CR, and CB, respectively) in the ACC of PBS-treated WT. **(B)** Micrographs show double labeling for 8-oxo-dG and three interneuron markers (PV, CR, and CB, respectively) in the ACC of PBS-treated and GBR-treated *Gclm* KO mice. Scale: 10 μm. **(C)** Quantification reveals a high amount of 8-oxo-dG labeling in PVI (left graph) but not in CRI (middle graph) and in CBI (right graph). The amount of 8-oxo-dG labeling in an interneuron type is given by the percentage (± SD) of voxels labeled with a specific interneuron marker, which are co-labeled with 8-oxo-dG. The 8-oxo-dG labeling in PVI but not in CRI or CBI varies significantly with genotype [$F(1,15) = 15.31$, $p = .002$] and GBR treatment [$F(1,15) = 17.47$, $p = .001$, two-way analysis of variance, $n = 4$ in each group]. $^{**}p < .01$. The insert illustrates the experimental design. The red horizontal line indicates the treatment period; the arrowhead indicates the time of sacrifice at P20. Abbreviations as in Figures 1 and 2.

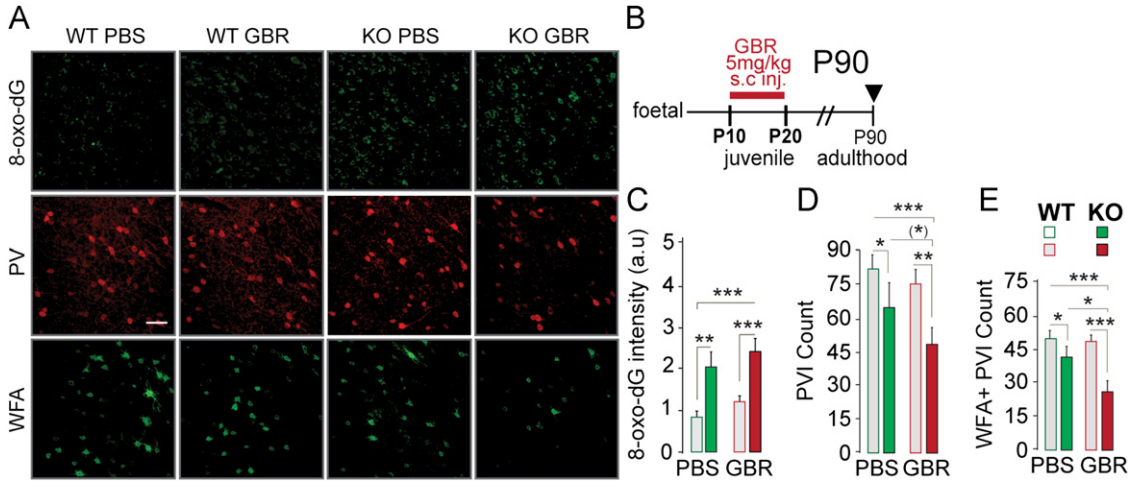

Figure 5. Long-term effects of GBR administration during preweaning age on 8-oxo-dG, PVI, and PNN in the ACC of young adult (P90) *Gclm* KO and WT mice. **(A)** Micrographs show labeling for 8-oxo-dG, PV, and WFA (labels PNN) in the ACC of adult WT and *Gclm* KO mice treated with either PBS or GBR during preweaning age. Scale: 50 μm. **(B)** Experimental design illustrating the preweaning treatment (from P10 to 20, red horizontal line) and the time of sacrifice at P90 (black arrowhead). **(C)** The 8-oxo-dG labeling (in a.u.) is significantly higher in *Gclm* KO compared with WT mice [analysis of variance, $F(1,15) = 51.47$, $p < .0001$], irrespective of treatment. For each group, $n = 4–5$. **(D)** The GBR and PBS treatments during preweaning age significantly decrease PVI number in *Gclm* KO compared with WT mice. The effect tends to be stronger after GBR compared with PBS treatment. For each group, $n = 4–5$. **(E)** The GBR and PBS treatments during preweaning age decrease PNN (WFA + PVI) in *Gclm* KO compared with WT mice. The effect is significantly stronger after GBR compared with PBS treatment. For each group, $n = 4–5$. Bars in all graphs represent SD. ***$p < .001$; **$p < .01$; *$p < .05$, (*)$p = .08$. Abbreviations as in Figures 1 and 2.

Discussion

This study reveals that, compared with CB or CR interneurons, PVI in the ACC are sensitive to a redox dysregulation and are prone to exhibit oxidative stress. Parvalbumin-expressing fast-spiking interneurons are more sensitive to oxidative stress during early postnatal development than during adulthood. A GSH deficit (as in *Gclm* KO), which leads to increase in oxidative stress, is sufficient to delay PVI maturation and PNN formation. When the compromised redox system is further challenged at preweaning and pubertal ages by an additional oxidative stress (i.e., due to excess of extracellular dopamine induced by the dopamine reuptake inhibitor GBR), PVI integrity is also affected. This PVI impairment induced in young KO mice persists in adulthood. By contrast, PVI in KO mice are more resistant to an additional oxidative stress if applied during young adulthood. Finally, preventing oxidative stress with the antioxidant and redox regulator NAC protects PVI and PNN.

The vulnerability of PVI in KO mice is associated with a predisposition of these interneurons to exhibit oxidative stress most likely at mitochondrial DNA level, as suggested by the extranuclear 8-oxo-dG labeling. Mitochondria are, among organelles and subcellular compartments, most susceptible to oxidation under stressed conditions (57). Sensitivity to oxidative stress predominates in PVI compared with other interneurons, such as CB- and CR-expressing interneurons. This could be explained by the high metabolic requirement of their fast-spiking properties (58). But the vulnerability of PVI in ACC of KO mice varies as a function of age, with the most sensitive period being at preweaning and pubertal stages, and the least sensitive one during early adulthood. During the vulnerability period, the PNN surrounding most PVI are not yet fully formed. A lack of mature PNN around PVI might contribute to the vulnerability of these interneurons during their development, because PNN protects cells against oxidative stress (59). By contrast, the presence of well-formed PNN in young adults might limit oxidative stress generated by GBR and therefore protect PVI. Along this line, the delayed maturation of PNN in KO mice could extend the vulnerability of PVI to oxidative stress over a prolonged period of postnatal development. The cause for the delayed formation of PNN is unknown. The PNN formation requires neuronal activity and calcium influx via α-amino-3-hydroxy-5-methyl-4-isoxazole propionic acid receptors and L-type channels (60,61). Oxidative conditions and GSH deficit could affect intracellular calcium homeostasis, because *N*-methyl-D-aspartate receptors, L-type calcium channels, ryanodine, and IP3 receptors are all modulated by the redox status (62–66).

Another significant finding is that oxidative stress, resulting from genetically induced GSH deficit combined with an exogenous stress applied during postnatal development, has long-lasting effects on PVI. The PVI in the ACC of KO mice are very sensitive to early-life disturbance, because even a daily subcutaneous injection of physiological solution during preweaning age—which might constitute a stressful event—causes PVI impairment in adults. The long-term PVI defect that we observed resembles the long-term blockade of PVI maturation (without cell death) after an early postnatal ketamine treatment known to generate high amounts of superoxide (67). By abolishing oxidative stress, NAC protects PVI of KO mice against the deleterious effect of GBR. The protection by NAC might be mediated by its own antioxidant redox regulator properties. Indeed, NAC treatment did not increase brain GSH in young KO mice, because they have a deficient GSH synthesis (37). Thus, in mice with a compromised $(GSH)_2$/GSH redox cycle, NAC could provide an additional source of cysteine (Cys), required for the $(Cys)_2$/Cys redox cycle to act as an alternative mechanism for preventing oxidative stress and maintaining an appropriate intracellular thiol redox state (68). In addition, NAC has anti-inflammatory properties, which could minimize the inflammation-mediated impairment of PVI (21). Indeed, there is positive feedback between

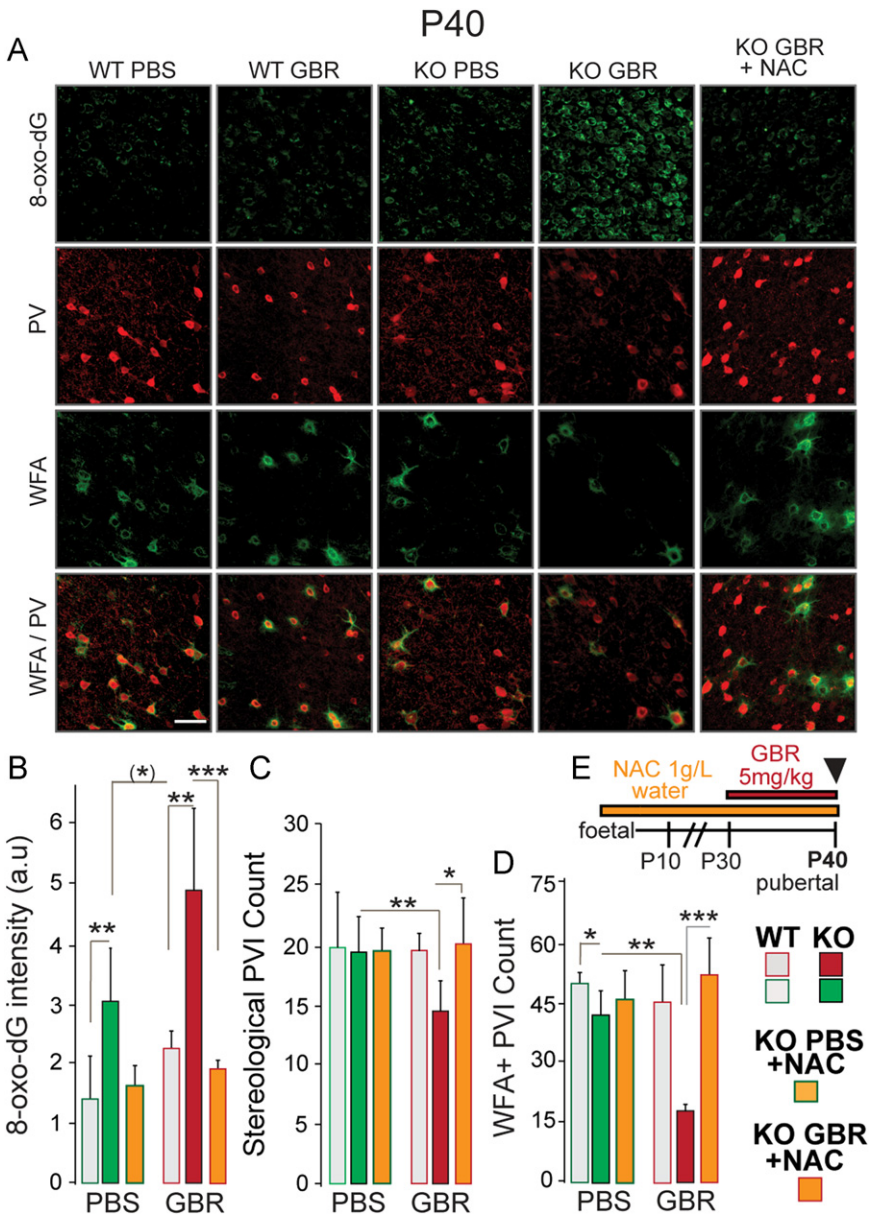

Figure 6. *N*-acetylcysteine (NAC) protects PVI against GBR-induced oxidative stress. **(A)** Micrographs show labeling for 8-oxo-dG, PV, and WFA (labels PNN) in the ACC of WT and *Gclm* KO mice treated with either PBS or GBR during the pubertal period in absence or presence of NAC treatment. Scale: 40 μm. **(B)** NAC prevents the GBR-induced increase in 8-oxo-dG labeling. **(C)** Stereological quantification reveals that NAC prevents the GBR-induced decrease of PVI number in *Gclm* KO mice. **(D)** NAC prevents the GBR-induced (not PBS-induced) decrease of PNN (WFA + PVI) in *Gclm* KO mice. Bars in all graphs represent SD. For each group, $n = 5$. ***$p < .001$; **$p < .01$; *$p < .05$; (*)$p = .07$. **(E)** Experimental design. The red horizontal line indicates the GBR treatment period (from P30 to 40); the orange horizontal line illustrates the period of NAC treatment; the arrowhead indicates the time of sacrifice at day 40 (P40). Abbreviations as in Figures 1 and 2.

oxidative stress and inflammatory processes, and increasing evidence also point to a subclinical inflammatory-like state in schizophrenia (69,70).

The present study reveals that—compared with another region investigated, the hippocampus (38)—the ACC is particularly prone to oxidative stress during early postnatal development. Significant oxidative stress is observed in the ACC of young preweaning KO mice. By contrast, the ventral hippocampus only starts to display oxidative stress during pubertal age, whereas the dorsal hippocampus does not exhibit a significant level of oxidative stress even in fully adult KO mice (38). Thus, the ACC could be highly vulnerable to early insults. The resulting redox dysregulation during this critical period could contribute to abnormal development and maturation of this prefrontal area. Data from animals and humans indicate that early-life stress affects durably the ACC (40–43). A recent study shows that the activation of the perigenual ACC during a cognitive task under time and social pressure was positively correlated with urban upbringing (71), suggesting that early stresses associated with urban life can modify the ACC function. Together with being born and brought up in a city, childhood trauma (emotional, physical, and sexual abuses) are associated with increased risk for psychosis (72–75). It is therefore plausible that the impact of early-life environmental stressful conditions on the ACC, a brain region affected in patients, might contribute to the emergence of schizophrenia, particularly in genetically vulnerable individuals.

Altogether, our data provide new insights into how the convergence of genetic and environmental risk factors, occurring at specific times during development, could potentially contribute via redox dysregulation mechanisms to PVI dysfunction. Many environmental insults, known to be risk factors for schizophrenia, generate oxidative stress and affect the antioxidant systems of the brain, including the GSH system (1). There is also evidence for a genetic origin of redox dysregulation involving the GSH system in subgroups of patients (6,76). Several vulnerability genes (*PRODH, DISC-1, G72, dysbindin*) for schizophrenia and/or

bipolar disease might also be associated with a redox dysregulation, because anomalies of the encoded proteins lead to mitochondrial or antioxidant dysfunction (7–11). Early-life environmental insults inducing oxidative stress could therefore be detrimental to nonmature PVI and have enduring consequences, resulting in neuronal synchrony impairment and cognitive deficits. Individuals carrying a genetic predisposition to redox dysregulation would be highly vulnerable during the maturation of PVI. Finally, our data provide support for the need to develop novel therapeutic approaches based on antioxidant and redox regulator compounds that could be used preventively in young at-risk subjects.

This work was supported by the Swiss National Science Foundation (#31-116689 to KQD and #310030_135736/1 to KQD and PS), "Loterie Romande", Damm-Etienne Foundation, and Alamaya Foundation. We thank Adeline Cottier for her technical assistance and Ying Chen and Timothy Dalton for kindly providing us the Gclm KO mice.

The authors report no biomedical financial interests or potential conflicts of interest.

Supplementary material cited in this article is available online.

1. Do KQ, Cabungcal JH, Frank A, Steullet P, Cuenod M (2009): Redox dysregulation, neurodevelopment, and schizophrenia. *Curr Opin Neurobiol* 19:220–230.
2. Yao JK, Keshavan MS (2011): Antioxidants, redox signaling, and pathophysiology in schizophrenia: An integrative view. *Antioxid Redox Signal* 15:2011–2035.
3. Berk M, Copolov D, Dean O, Lu K, Jeavons S, Schapkaitz I, *et al*. (2008): N-acetyl cysteine as a glutathione precursor for schizophrenia—a double-blind, randomized, placebo-controlled trial. *Biol Psychiatry* 64: 361–368.
4. Carmeli C, Knyazeva MG, Cuenod M, Do KQ (2012): Glutathione precursor N-acetyl-cysteine modulates EEG synchronization in schizophrenia patients: A double-blind, randomized, placebo-controlled trial. *PLoS One* 7:e29341.
5. Lavoie S, Murray MM, Deppen P, Knyazeva MG, Berk M, Boulat O, *et al*. (2008): Glutathione precursor, N-acetyl-cysteine, improves mismatch negativity in schizophrenia patients. *Neuropsychopharmacology* 33: 2187–2199.
6. Gysin R, Kraftsik R, Sandell J, Bovet P, Chappuis C, Conus P, *et al*. (2007): Impaired glutathione synthesis in schizophrenia: Convergent genetic and functional evidence. *Proc Natl Acad Sci U S A* 104: 16621–16626.
7. Gokhale A, Larimore J, Werner E, So L, Moreno-De-Luca A, Lese-Martin C, *et al*. (2012): Quantitative proteomic and genetic analyses of the schizophrenia susceptibility factor dysbindin identify novel roles of the biogenesis of lysosome-related organelles complex 1. *J Neurosci* 32: 3697–3711.
8. Goldshmit Y, Erlich S, Pinkas-Kramarski R (2001): Neuregulin rescues PC12-ErbB4 cells from cell death induced by H(2)O(2). Regulation of reactive oxygen species levels by phosphatidylinositol 3-kinase. *J Biol Chem* 276:46379–46385.
9. Krishnan N, Dickman MB, Becker DF (2008): Proline modulates the intracellular redox environment and protects mammalian cells against oxidative stress. *Free Radic Biol Med* 44:671–681.
10. Otte DM, Sommersberg B, Kudin A, Guerrero C, Albayram O, Filiou MD, *et al*. (2011): N-acetyl cysteine treatment rescues cognitive deficits induced by mitochondrial dysfunction in G72/G30 transgenic mice. *Neuropsychopharmacology* 36:2233–2243.
11. Park YU, Jeong J, Lee H, Mun JY, Kim JH, Lee JS, *et al*. (2010): Disrupted-in-schizophrenia 1 (DISC1) plays essential roles in mitochondria in collaboration with Mitofilin. *Proc Natl Acad Sci U S A* 107: 17785–17790.
12. Lewis DA, Levitt P (2002): Schizophrenia is a disorder of neurodevelopment. *Annu Rev Neurosci* 25:409–432.
13. Lewis DA, Curley AA, Glausier JR, Volk DW (2012): Cortical parvalbumin interneurons and cognitive dysfunction in schizophrenia. *Trends Neurosci* 35:57–67.
14. Bartos M, Vida I, Jonas P (2007): Synaptic mechanisms of synchronized gamma oscillations in inhibitory interneuron networks. *Nat Rev Neurosci* 8:45–56.
15. Sohal VS, Zhang F, Yizhar O, Deisseroth K (2009): Parvalbumin neurons and gamma rhythms enhance cortical circuit performance. *Nature* 459:698–702.
16. Whittington MA, Cunningham MO, LeBeau FE, Racca C, Traub RD (2011): Multiple origins of the cortical gamma rhythm. *Dev Neurobiol* 71:92–106.
17. Barr MS, Farzan F, Tran LC, Chen R, Fitzgerald PB, Daskalakis ZJ (2010): Evidence for excessive frontal evoked gamma oscillatory activity in schizophrenia during working memory. *Schizophr Res* 121:146–152.
18. Cho RY, Konecky RO, Carter CS (2006): Impairments in frontal cortical gamma synchrony and cognitive control in schizophrenia. *Proc Natl Acad Sci U S A* 103:19878–19883.
19. Spencer KM, Niznikiewicz MA, Shenton ME, McCarley RW (2008): Sensory-evoked gamma oscillations in chronic schizophrenia. *Biol Psychiatry* 63:744–747.
20. Uhlhaas PJ, Singer W (2011): The development of neural synchrony and large-scale cortical networks during adolescence: Relevance for the pathophysiology of schizophrenia and neurodevelopmental hypothesis. *Schizophr Bull* 37:514–523.
21. Brenhouse HC, Andersen SL (2011): Nonsteroidal anti-inflammatory treatment prevents delayed effects of early life stress in rats. *Biol Psychiatry* 70:434–440.
22. Schiavone S, Sorce S, Dubois-Dauphin M, Jaquet V, Colaianna M, Zotti M, *et al*. (2009): Involvement of NOX2 in the development of behavioral and pathologic alterations in isolated rats. *Biol Psychiatry* 66:384–392.
23. Harte MK, Powell SB, Swerdlow NR, Geyer MA, Reynolds GP (2007): Deficits in parvalbumin and calbindin immunoreactive cells in the hippocampus of isolation reared rats. *J Neural Transm* 114:893–898.
24. Behrens MM, Ali SS, Dao DN, Lucero J, Shekhtman G, Quick KL, *et al*. (2007): Ketamine-induced loss of phenotype of fast-spiking interneurons is mediated by NADPH-oxidase. *Science* 318:1645–1647.
25. Do KQ, Trabesinger AH, Kirsten-Kruger M, Lauer CJ, Dydak U, Hell D, *et al*. (2000): Schizophrenia: Glutathione deficit in cerebrospinal fluid and prefrontal cortex in vivo. *Eur J Neurosci* 12:3721–3728.
26. Gawryluk JW, Wang JF, Andreazza AC, Shao L, Young LT (2011): Decreased levels of glutathione, the major brain antioxidant, in postmortem prefrontal cortex from patients with psychiatric disorders. *Int J Neuropsychopharmacol* 14:123–130.
27. Wang JF, Shao L, Sun X, Young LT (2009): Increased oxidative stress in the anterior cingulate cortex of subjects with bipolar disorder and schizophrenia. *Bipolar Disord* 11:523–529.
28. Hashimoto T, Volk DW, Eggan SM, Mirnics K, Pierri JN, Sun Z, *et al*. (2003): Gene expression deficits in a subclass of GABA neurons in the prefrontal cortex of subjects with schizophrenia. *J Neurosci* 23:6315–6326.
29. Beasley CL, Zhang ZJ, Patten I, Reynolds GP (2002): Selective deficits in prefrontal cortical GABAergic neurons in schizophrenia defined by the presence of calcium-binding proteins. *Biol Psychiatry* 52:708–715.
30. Dell'Anna E, Geloso MC, Magarelli M, Molinari M (1996): Development of GABA and calcium binding proteins immunoreactivity in the rat hippocampus following neonatal anoxia. *Neurosci Lett* 211:93–96.
31. Jiang M, Swann JW (2005): A role for L-type calcium channels in the maturation of parvalbumin-containing hippocampal interneurons. *Neuroscience* 135:839–850.
32. Pangratz-Fuehrer S, Hestrin S (2011): Synaptogenesis of electrical and GABAergic synapses of fast-spiking inhibitory neurons in the neocortex. *J Neurosci* 31:10767–10775.
33. Tseng KY, O'Donnell P (2007): Dopamine modulation of prefrontal cortical interneurons changes during adolescence. *Cereb Cortex* 17: 1235–1240.
34. Wang HX, Gao WJ (2010): Development of calcium-permeable AMPA receptors and their correlation with NMDA receptors in fast-spiking interneurons of rat prefrontal cortex. *J Physiol* 588:2823–2838.
35. Hartig W, Brauer K, Bigl V, Bruckner G (1994): Chondroitin sulfate proteoglycan-immunoreactivity of lectin-labeled perineuronal nets around parvalbumin-containing neurons. *Brain Res* 635:307–311.
36. Kwok JC, Dick G, Wang D, Fawcett JW (2011): Extracellular matrix and perineuronal nets in CNS repair. *Dev Neurobiol* 71:1073–1089.

37. Duarte JM, Kulak A, Gholam-Razaee MM, Cuenod M, Gruetter R, Do KQ (2012): *N*-acetylcysteine normalizes neurochemical changes in the glutathione-deficient schizophrenia mouse model during development. *Biol Psychiatry* 71:1006–1014.
38. Steullet P, Cabungcal JH, Kulak A, Kraftsik R, Chen Y, Dalton TP, *et al*. (2010): Redox dysregulation affects the ventral but not dorsal hippocampus: Impairment of parvalbumin neurons, gamma oscillations, and related behaviors. *J Neurosci* 30:2547–2558.
39. Tosic M, Ott J, Barral S, Bovet P, Deppen P, Gheorghita F, *et al*. (2006): Schizophrenia and oxidative stress: Glutamate cysteine ligase modifier as a susceptibility gene. *Am J Hum Genet* 79:586–592.
40. Cohen RA, Grieve S, Hoth KF, Paul RH, Sweet L, Tate D, *et al*. (2006): Early life stress and morphometry of the adult anterior cingulate cortex and caudate nuclei. *Biol Psychiatry* 59:975–982.
41. Gos T, Bock J, Poeggel G, Braun K (2008): Stress-induced synaptic changes in the rat anterior cingulate cortex are dependent on endocrine developmental time windows. *Synapse* 62:229–232.
42. Law AJ, Pei Q, Feldon J, Pryce CR, Harrison PJ (2009): Gene expression in the anterior cingulate cortex and amygdala of adolescent marmoset monkeys following parental separations in infancy. *Int J Neuropsychopharmacol* 12:761–772.
43. Thomaes K, Dorrepaal E, Draijer N, de Ruiter MB, van Balkom AJ, Smit JH, *et al*. (2010): Reduced anterior cingulate and orbitofrontal volumes in child abuse-related complex PTSD. *J Clin Psychiatry* 71:1636–1644.
44. Fornito A, Yücel M, Dean B, Wood SJ, Pantelis C (2009): Anatomical abnormalities of the anterior cingulate cortex in schizophrenia: Bridging the gap between neuroimaging and neuropathology. *Schizophr Bull* 35:973–993.
45. Todtenkop MS, Vincent SL, Benes FM (2005): A cross-study meta-analysis and three-dimensional comparison of cell counting in the anterior cingulate cortex of schizophrenic and bipolar brain. *Schizophr Res* 73:79–89.
46. Yang Y, Dieter MZ, Chen Y, Shertzer HG, Nebert DW, Dalton TP (2002): Initial characterization of the glutamate-cysteine ligase modifier subunit Gclm(-/-) knockout mouse. Novel model system for a severely compromised oxidative stress response. *J Biol Chem* 277:49446–49452.
47. Atkuri KR, Mantovani JJ, Herzenberg LA, Herzenberg LA (2007): *N*-acetylcysteine—a safe antidote for cysteine/glutathione deficiency. *Curr Opin Pharmacol* 7:355–359.
48. Cabungcal JH, Nicolas D, Kraftsik R, Cuenod M, Do KQ, Hornung JP (2006): Glutathione deficit during development induces anomalies in the rat anterior cingulate GABAergic neurons: Relevance to schizophrenia. *Neurobiol Dis* 22:624–637.
49. Franklin BJ, Paxinos G (2008): *The Mouse Brain in Stereotaxic Coordinates*, *3rd ed.* New York: Academic Press Elsevier.
50. Schmitz C, Hof PR (2005): Design-based stereology in neuroscience. *Neuroscience* 130:813–831.
51. Kasai H (1997): Analysis of a form of oxidative DNA damage, 8-hydroxy-2′-deoxyguanosine, as a marker of cellular oxidative stress during carcinogenesis. *Mutat Res* 387:147–163.
52. Cadet JL, Brannock C (1998): Free radicals and the pathobiology of brain dopamine systems. *Neurochem Int* 32:117–131.
53. Rabinovic AD, Hastings TG (1998): Role of endogenous glutathione in the oxidation of dopamine. *J Neurochem* 71:2071–2078.
54. Feenstra MG, Vogel M, Botterblom MH, Joosten RN, de Bruin JP (2001): Dopamine and noradrenaline efflux in the rat prefrontal cortex after classical aversive conditioning to an auditory cue. *Eur J Neurosci* 13:1051–1054.
55. Lataster J, Collip D, Ceccarini J, Haas D, Booij L, van OJ, *et al*. (2011): Psychosocial stress is associated with in vivo dopamine release in human ventromedial prefrontal cortex: A positron emission tomography study using [(18)F]fallypride. *Neuroimage* 58:1081–1089.
56. Rivera A, Peňafiel A, Megías M, Agnati LF, López-Tèllez JF, Gago B, *et al*. (2008): Cellular localization and distribution of dopamine D_4 receptors in the rat cerebral cortex and their relationship with the cortical dopaminergic and noradrenergic nerve terminal networks. *Neuroscience* 155:997–1010.
57. Jones DP, Go YM (2010): Redox compartmentalization and cellular stress. *Diabetes Obes Metab* 12(suppl 2):116–125.
58. Hasenstaub A, Otte S, Callaway E, Sejnowski TJ (2010): Metabolic cost as a unifying principle governing neuronal biophysics. *Proc Natl Acad Sci U S A* 107:12329–12334.
59. Cabungcal JH, Steullet P, Kraftsik R, Cuenod M, Do QK (2011): The perineuronal net protects parvalbumin-immunoreactive interneurons against oxidative stress: Relevance to schizophrenia. Meeting of the Society for Neuroscience, November 12-16, 2011, Washington, DC. Available at: www.sfn.org/AM2011/, Meeting Planner Abstract 679.26/DD15. Accessed October 29, 2012.
60. Bruckner G, Grosche J (2001): Perineuronal nets show intrinsic patterns of extracellular matrix differentiation in organotypic slice cultures. *Exp Brain Res* 137:83–93.
61. Dityatev A, Bruckner G, Dityateva G, Grosche J, Kleene R, Schachner M (2007): Activity-dependent formation and functions of chondroitin sulfate-rich extracellular matrix of perineuronal nets. *Dev Neurobiol* 67: 570–588.
62. Bull R, Finkelstein JP, Humeres A, Behrens MI, Hidalgo C (2007): Effects of ATP, Mg2+, and redox agents on the Ca2+ dependence of RyR channels from rat brain cortex. *Am J Physiol Cell Physiol* 293: C162–C171.
63. Campbell DL, Stamler JS, Strauss HC (1996): Redox modulation of L-type calcium channels in ferret ventricular myocytes. Dual mechanism regulation by nitric oxide and S-nitrosothiols. *J Gen Physiol* 108: 277–293.
64. Choi Y, Chen HV, Lipton SA (2001): Three pairs of cysteine residues mediate both redox and zn2+ modulation of the nmda receptor. *J Neurosci* 21:392–400.
65. Joseph SK, Nakao SK, Sukumvanich S (2006): Reactivity of free thiol groups in type-I inositol trisphosphate receptors. *Biochem J* 393: 575–582.
66. Steullet P, Lavoie S, Kraftsik R, Guidi R, Gysin R, Cuenod M, *et al*. (2008): A glutathione deficit alters dopamine modulation of L-type calcium channels via D2 and ryanodine receptors in neurons. *Free Radic Biol Med* 44:1042–1054.
67. Powell SB, Sejnowski TJ, Behrens MM (2012): Behavioral and neurochemical consequences of cortical oxidative stress on parvalbumin-interneuron maturation in rodent models of schizophrenia. *Neuropharmacology* 62:2322–2331.
68. Mandal PK, Seiler A, Perisic T, Kolle P, Banjac CA, Forster H, *et al*. (2010): System x(c)- and thioredoxin reductase 1 cooperatively rescue glutathione deficiency. *J Biol Chem* 285:22244–22253.
69. Potvin S, Stip E, Sepehry AA, Gendron A, Bah R, Kouassi E (2008): Inflammatory cytokine alterations in schizophrenia: A systematic quantitative review. *Biol Psychiatry* 63:801–808.
70. Saetre P, Emilsson L, Axelsson E, Kreuger J, Lindholm E, Jazin E (2007): Inflammation-related genes up-regulated in schizophrenia brains. *BMC Psychiatry* 7:46.
71. Lederbogen F, Kirsch P, Haddad L, Streit F, Tost H, Schuch P, *et al*. (2011): City living and urban upbringing affect neural social stress processing in humans. *Nature* 474:498–501.
72. Brown AS (2011): The environment and susceptibility to schizophrenia. *Prog Neurobiol* 93:23–58.
73. Conus P, Cotton S, Schimmelmann BG, McGorry PD, Lambert M (2010): Pretreatment and outcome correlates of sexual and physical trauma in an epidemiological cohort of first-episode psychosis patients. *Schizophr Bull* 36:1105–1114.
74. Krabbendam L, van Os J (2005): Schizophrenia and urbanicity: A major environmental influence—conditional on genetic risk. *Schizophr Bull* 31:795–799.
75. Schafer I, Fisher HL (2011): Childhood trauma and posttraumatic stress disorder in patients with psychosis: Clinical challenges and emerging treatments. *Curr Opin Psychiatry* 24:514–518.
76. Gysin R, Kraftsik R, Boulat O, Bovet P, Conus P, Comte-Krieger E, *et al*. (2011): Genetic dysregulation of glutathione synthesis predicts alteration of plasma thiol redox status in schizophrenia. *Antioxid Redox Signal* 15:2003–2010.